

NUMERICAL COMPUTATION OF THE SOUND RADIATION FROM A PLANAR BAFFLED VIBRATING SURFACE

JORGE P. ARENAS

*Institute of Acoustics, Universidad Austral de Chile
Campus Miraflores, Edificio 6000
P.O. Box 567, Valdivia, Chile
jparenas@uach.cl*

Received 11 January 2007

Revised 12 October 2007

The sound power radiated by a plane vibrating structure can be calculated by numerical integration of the Rayleigh integral or by means of finite and boundary element methods. However, these methods are usually time-consuming due to the numerical evaluation of surface integrals. This paper reviews and discusses an alternative numerical method (the lumped parameter model) to compute the sound radiation from planar structures which is based just on surface velocity information and a direct numerical evaluation of the radiation resistance matrix of the structure. As an example, the technique is applied to estimate the sound radiated from the structural axisymmetric modes of both clamped and simply-supported circular baffled plates.

Keywords: Sound radiation; resistance matrix; radiation modes.

1. Introduction

The vibration of a plate's surface and its interaction with the fluid medium results in the radiation of sound and a coupled vibro-acoustic problem. The staggered method has been used to solve the fluid–structure interaction problem in the time domain. In this method both fluid and structure have to be integrated in time simultaneously.¹

In recent years, with the practical application of active sound and vibration control, several studies have been devoted to estimate the sound radiation characteristics of plates subject to different kinds of excitation and with various boundary conditions. The sound power radiated by a plate can be calculated if its surface response is known. However, this makes it necessary to determine the acoustic field by using the Rayleigh integral (for the sound pressure distribution) and then to perform an integration over a closed control surface.² Green functions can be theoretically derived for certain regular geometries. But for a complex and irregular geometric shape, or for a sound-radiating body not located in a free field, the function takes very complicated forms which are not easily determined mathematically.

As computer resources become less expensive and more readily available, it is becoming increasingly practical to use computational methods to predict the propagation and

radiation of sound and the behavior of complex structural systems. An excellent review of the numerical techniques used to predict low-frequency sound radiation has been presented by Atalla and Bernhard.³ Usually, for low frequencies, the sound power is calculated using the data obtained from a finite mesh on the structural surface for which the vibration velocities have been computed. Subsequently, the sound power is computed using the boundary element method.⁴ In general, the mesh needed to compute the sound radiation need not be as fine as the mesh needed to calculate the structural vibration. Therefore, sometimes acoustical analysis can be very inefficient.⁵ Some authors⁶ have shown that adaptivity can provide an increase in mesh efficiency for the Helmholtz problems at moderate wave numbers. On the other hand, the variational boundary element method requires evaluation of double surface integrals which makes the method time-consuming. An acceleration technique based on multipole expansion has been presented by Tournour and Atalla.⁷

In a complicated structure, the total sound field is composed of several vibrating substructures, each one producing a particular radiated sound power. Identification of these substructures can be achieved by sound intensity measurements with two closely-spaced microphones to measure the sound pressure and to estimate the particle velocity. However, this classical method has some practical limitations.⁸

The Rayleigh integral has been used as an alternative to the finite/boundary elements solution of an acoustic boundary problem. The Rayleigh integral is an approximate radiation integral in which it is assumed that the vibrating surface is flat or near flat, and lies in an infinite, reflecting baffle. In particular, applications of the Rayleigh integral to calculate the sound radiation from the structural modes of plates having different shapes and boundary conditions, have been reported by several investigators.^{9–11} An application to structural–acoustic optimization can be found in the work by Wodtke and Lamancusa.¹² They presented a research on sound power minimization of circular plates through a redistribution of unconstrained damping layers. In their work, the vibration analysis was based on the finite-element method, and here the acoustic radiation was treated by means of the Rayleigh integral. In general, the sound field radiated is obtained through applying a direct numerical integration scheme to the Rayleigh integral. Kirkup¹¹ introduced a method that is derived through numerical product integration of the Rayleigh integral. He observed that the integrand of the Rayleigh integral can be singular or near-singular, and it can become increasingly oscillatory as the wavenumber increases. Therefore, the direct numerical integration can be computationally inefficient sometimes.

A discrete approach that can be used to estimate the sound power radiated from a structure can be based on the acoustic radiation resistance matrix. A practical application of the acoustic radiation resistance matrix was presented by Paddock and Koopmann¹³ to assess the noise characteristics of machines. However, this matrix has been mainly used for active structural acoustical control of low-frequency noise radiated by vibrating structures.¹⁴

Associated to the radiation resistance matrix are the radiation modes. These modes are related with surface velocity distributions that produce orthogonal sound pressure radiation fields. Considerable research has been devoted to these topics in the last 17 years.

The radiation mode technique has a number of parallels to the usual modal analysis and thus many analogies can be formulated.

The origins of the radiation mode technique can be found in a seminal study by Borgiotti¹⁵ on the determination of the sound power radiated by a vibrating body submerged in a fluid from boundary measurements. The study is based on the singular function analysis of the radiator operator and the singular value decomposition (SVD) of its matrix discrete representation. In fact, Borgiotti's work appears as the first to employ this algorithm. His analysis leads to the decomposition of the boundary normal velocity into efficient and inefficient components, where the inefficient components are associated with very weakly radiating evanescent fields. Thus, source modes that are eigenstates of radiated power are identified and later applied to radiation filtering. In a following paper, Photiadis¹⁶ discussed the close relationship between SVD filtering and the well-known wave vector filtering. In particular, he showed that the efficiently radiating modes correspond approximately to supersonic surface wave numbers, and the weakly radiating modes correspond to subsonic wave numbers.

A different algorithm¹⁷ to identify the same states, which does not require the application of the SVD, consists of computing the eigenstates of the surface acoustic resistance, where its eigenvalues are proportional to the radiated power.

Cunefare¹⁸ presented a paper discussing a technique for deriving the optimal surface velocity distribution on the surface of a finite baffled beam. The technique considers the optimal situation of radiated sound power under a certain constraint, which leads to a problem identical in form to the symmetric eigenvalue problem of the Rayleigh quotient employed in dynamical mechanical systems. Here, it can be observed that the eigenvectors form an orthonormal set of basis functions for representing the surface normal velocity. On the other hand, the eigenvalues are associated to the sound radiation efficiencies. Numerical examples were presented for simply-supported and clamped-clamped boundary conditions. Later, Cunefare and Currey¹⁹ studied the Rayleigh quotient formulation to investigate convergence, bounding, and sensitivity of the radiation modes. It is worth noticing that the term "radiation modes" seems to be introduced first by Cunefare in 1990.²⁰

A study on complex power, reciprocity, and radiation modes for submerged bodies surrounded by heavy acoustic fluid has been reported by Chen and Ginsberg.²¹ They used the radiation modes to form modal series for the surface pressure and normal velocity due to a specified excitation. The theory was applied to an example for a slender spheroidal body to evaluate the radiation mode patterns in a range of frequencies.

Fahnline and Koopmann²² defined a "lumped parameter model" for the acoustic radiation from a vibrating structure by dividing its surface into elements, expanding the acoustic field from each of the elements in a multipole expansion, and then truncating all but the lowest-order terms in the expansion. Later, they implemented numerically the model by requiring the boundary condition for the normal surface velocity to be satisfied in a lumped parameter sense.²³ The basis functions for the numerical analysis were taken as the acoustic fields of discrete monopole, dipole, and tripole sources located at the geometrical centers of

the surface elements. However, a disadvantage of the method was the amount of computational time spent in solving the system of equations for the source amplitudes. A technique to overcome this problem has been reported by Fahnline.⁵

As noted in the review by Marburg,²⁴ the lumped parameter model is similar to the model named “direct finite-element method” presented by Hubner,²⁵ which also uses simplified representations of the particle velocity distribution on the body surface. Both methods provide identical solutions although they involve different assumptions.

More recently, Maury and Elliott²⁶ have presented analytical approximations for the radiation modes of a baffled rectangular panel in terms of prolate spheroidal wave functions. They established these approximations by observing the similarity between the problem of determining the radiation modes of a structure in a system of rectangular coordinates and the so-called concentration problem which is found in electrical engineering. These approximations were used to determine upper bounds on the number of radiation modes that could be actively canceled in order to reduce the sound power radiated from planar rectangular structures.

In recent years, a large body of literature has been dedicated to the application of structural optimization for passive noise control. Structural–acoustic optimization is understood as an iterative minimum search of a specified cost function by modifying a set of design variables.²⁴ Examples of this are commonly found as applications to the reduction of sound radiation from both plates and shells. Fritze *et al.*²⁷ have presented a study on the reduction of sound power of plates and shallow shells by using simple local modification functions and a gradient-based method for optimization. The technique was applied to a simply-supported plate under harmonic sound pressure excitation. A comprehensive review of structural–acoustic optimization techniques has been presented by Marburg.²⁴

In a practical application, Kuijpers²⁸ presented three acoustic formulations to model the sound radiation of a magnetic resonance imaging (MRI) scanner: a semi-analytical formulation for the acoustic radiation of a finite duct with open ends mounted with infinite flanges, a Fourier boundary elements method, and the radiation modes formulation. In addition, he showed an enhancement to the radiation modes formulation which reduces the computational efforts in determining the radiation modes when only part of the outer geometry is radiating, i.e. an acoustic system with partly passive boundary condition. This development is quite helpful for MRI scanner acoustic design optimization. Subsequently, Kessels²⁹ studied the structural part of the MRI scanner noise radiation problem and the structural–acoustic optimization techniques for its low noise design.

An important body of literature on the application of the radiation modes can be found in the field of Active Structural–Acoustic Control (ASAC). In this technique the minimization of sound radiation is achieved by modifying the response of the structure through structural inputs using actuators.

A strategy for active control of the sound radiated from a structure that uses the radiation modes has been proposed by Naghshineh and Koopmann.³⁰ On the other hand, a scheme to estimate the true sound power radiated from a structure that makes use of the radiation modes and surface volume velocities was originally presented by Baumann *et al.*³¹

as *spatial filters*, and it has been implemented by Elliott and Johnson³² for very low frequencies. Additional developments have been reported by Currey and Cunefare,³³ Berkhoff,³⁴ and Bai and Tsao.³⁵ The combination of the acoustic radiation resistance matrix and the measurement of volume velocity by means of accelerometers on the surface of a rectangular plate has produced accurate prediction of the sound radiation efficiency.³⁶

In the following sections, the main mathematical fundamentals of the lumped parameter model and of the radiation modes are summarized. Then, as an academic example, the model is applied to a discretized circular geometry thus obtaining the radiation resistance matrix of the structure by direct numerical evaluation. Finally, the technique is applied to estimate the sound power radiated from the structural axisymmetric modes of a circular baffled plate having clamped and simply-supported rim. In addition, the sound efficiency of the radiation modes is calculated by means of an eigen-analysis of the resulting acoustic radiation resistance matrix.

2. Review of the Theory

2.1. Acoustic radiation resistance matrix

The acoustic radiation resistance matrix R_{ik} corresponds to a transfer function which relates the normal velocities of a vibrating structure to the sound pressures on its surface. This quantity is independent of the vibration and depends only on the geometry of the structure. The dimension of the matrix is given by the number of virtual subdivisions of the structure. We can define the local specific acoustic radiation impedance as the complex ratio between the sound pressure amplitude p_i at point i due to a point source located at point k , and the normal velocity V_{n_k} (see Fig. 1)

$$Z_{ik} = \left(\frac{p_i}{V_{n_k}} \right)_{\text{on } S}. \quad (1)$$

Now, the volume velocity is

$$u = \iint_S \mathbf{V} \cdot d\mathbf{S}. \quad (2)$$

Assuming that the characteristic length of the surface elements is small compared to a typical acoustic wavelength, the pressure and velocity can be considered constant over each element and can be represented by an average value. Therefore, Eq. (1) is

$$Z_{ik} = \frac{p_i}{u_k}, \quad (3)$$

and the acoustic radiation resistance matrix R_{ik} can be obtained by taking the real part of Z_{ik} .

A general solution for the problem of obtaining the R_{ik} can be found using the Kirchhoff-Helmholtz theorem. Let the boundary surface of a vibrating structure be divided into N elements of area S_k , with $k = 1, 2, \dots, N$. The sound pressure radiated at a point \mathbf{r} due

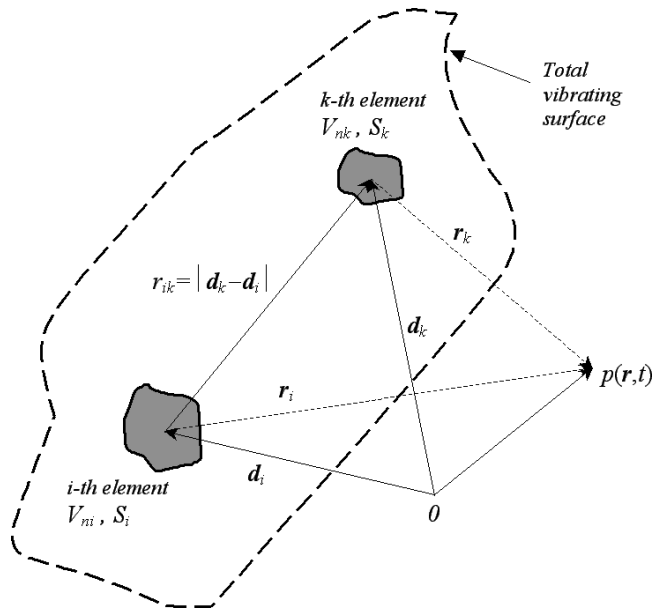


Fig. 1. Geometry for calculating the sound radiation from a vibrating surface.

to a surface element k located at a point \mathbf{r}_k and vibrating with surface velocity \mathbf{V} can be obtained using the Rayleigh integral³⁷

$$P(\mathbf{r}) = j \frac{\omega \rho_0}{4\pi} \iint_{S_k} \mathbf{V}(\mathbf{r}_k) G(\mathbf{r}|\mathbf{r}_k) \cdot d\mathbf{S}(\mathbf{r}_k), \quad (4)$$

where ω is the circular frequency, ρ_0 is the fluid density, $j = \sqrt{-1}$, and $G(\mathbf{r}|\mathbf{r}_k)$ is the Green's function of the second kind, which is equivalent to the field of a simple source in an infinite fluid medium. In addition, the Green's function satisfies the Neumann boundary condition on the surface. By definition, the average sound pressure over an element i of surface S_i is

$$p(\mathbf{r}_i) = \frac{1}{S_i} \iint_{S_i} P(\mathbf{r}_i) dS_i. \quad (5)$$

Then, substituting Eq. (4) into Eq. (5), we obtain

$$p(\mathbf{r}_i) = j \frac{\omega \rho_0}{4\pi S_i} \iint_{S_i} \iint_{S_k} \mathbf{V}(\mathbf{r}_k) G(\mathbf{r}_i|\mathbf{r}_k) \cdot d\mathbf{S}(\mathbf{r}_k) dS_i. \quad (6)$$

Assuming that each of the elements vibrates as a piston and that the Green's function can be considered approximately constant over each of the surface elements, we have that

$$p(\mathbf{r}_i) \sim j \frac{\omega \rho_0}{4\pi S_i} G(\mathbf{r}_i|\mathbf{r}_k) \iint_{S_i} dS_i \iint_{S_k} \mathbf{V}(\mathbf{r}_k) \cdot d\mathbf{S}(\mathbf{r}_k). \quad (7)$$

Using the definition of volume velocity from Eq. (2) and the definition of Z_{ik} from Eq. (3), R_{ik} can be approximated as

$$R_{ik} \sim -\frac{\omega\rho_0}{4\pi}\Im\{G(\mathbf{r}_i|\mathbf{r}_k)\}. \quad (8)$$

Theoretically, Green's function results are very convenient for deriving the sound pressure field produced by a vibrating source and to calculate the acoustic radiation matrix. However, the actual functional dependence of Green's function of the second kind is very difficult to predict for complex acoustical boundary value problems. Therefore, a discrete approach is more convenient in practice, particularly to determine the sound power radiated by the structure.

2.2. Matrix approach for the sound power radiated

The sound power radiated by a vibrating structure is a single global quantity commonly used to characterize its source strength. The time-averaged total sound power radiated $\bar{\Pi}_{\text{rad}}$ by a baffled plate's surface vibrating at a frequency ω is³⁸

$$\bar{\Pi}_{\text{rad}} = \frac{1}{2} \iint_S \Re\{p(\mathbf{r})V_n(\mathbf{r})^*\}dS, \quad (9)$$

where S is the total surface area of the plate, \mathbf{r} are the coordinates of the point on the surface, $p(\mathbf{r})$ is the complex sound pressure in the near field, $V_n(\mathbf{r})$ is the normal complex velocity on the plate, and $*$ denotes the complex conjugate. If the sound pressure is estimated from an integral representation, such as the Rayleigh integral, the evaluation of $\bar{\Pi}_{\text{rad}}$ requires to solve a quadruple integral.

A matrix approach can be obtained considering that the vibrating structure is divided into N small elements. Thus, combination of Eqs. (9), (2), and (3), yields¹³

$$\bar{\Pi}_{\text{rad}} = \frac{1}{4} \sum_{i=1}^N \sum_{k=1}^N Z_{ik}u_iu_k^* + \frac{1}{4} \sum_{i=1}^N \sum_{k=1}^N Z_{ik}^*u_i^*u_k. \quad (10)$$

Now, interchanging the indices and order in the summations, and after the application of the principle of reciprocity to acoustic fields $Z_{ik} = Z_{ki}$,³⁸ we obtain

$$\bar{\Pi}_{\text{rad}} = \frac{1}{2} \sum_{i=1}^N \sum_{k=1}^N R_{ik}u_iu_k^* = \frac{1}{2}\mathbf{u}^H\mathbf{R}\mathbf{u}, \quad (11)$$

where \mathbf{u} is the $N \times 1$ complex volume velocity vector, H denotes the Hermitian (conjugate transpose), and $R_{ik} = \Re\{Z_{ik}\}$ are the elements of the real $N \times N$ *acoustic radiation resistance matrix* \mathbf{R} , defined as

$$\mathbf{R} = \begin{bmatrix} R_{11} & R_{12} & \cdots & R_{1N} \\ R_{21} & R_{22} & \cdots & \vdots \\ \vdots & & \ddots & \vdots \\ R_{N1} & \cdots & \cdots & R_{NN} \end{bmatrix}. \quad (12)$$

Thus, Eq. (11) provides a convenient method to estimate the sound radiation for any assumed set of structural modes for a sound radiator of arbitrary shape. In the following sections, the term *resistance matrix* will be used to mean “acoustic radiation resistance matrix” in order to avoid a more lengthy adjectival phrase. Now, if we write the elements of \mathbf{u} as $u_i = |u_i|e^{j\phi_i}$, then

$$\bar{\Pi}_{\text{rad}} = \frac{1}{2} \sum_{i=1}^N R_{ii} |u_i|^2 + \frac{1}{2} \sum_{i=1}^N \sum_{\substack{k=1 \\ k \neq i}}^N R_{ik} |u_i| |u_k| \cos(\phi_k - \phi_i). \quad (13)$$

The first part on the right of Eq. (13) corresponds to the self-resistance and the second part is the cross-resistance, which gives a measure of the total acoustic coupling between the i th and k th surface elements. Therefore, the vector \mathbf{u} can be measured using the signals from accelerometers.³⁶ The resistance matrix can be measured using a resistance probe, or it can be evaluated analytically or numerically.

2.3. Sound radiation efficiency

A statistical-based measure of the average modal radiation resistance is commonly used to relate calculations or measurements of the mean square normal velocity, averaged over the radiating surface and the radiated power. It is called the radiation efficiency, or radiation ratio, and is defined as³⁸

$$\sigma_{\text{rad}} = \frac{\bar{\Pi}_{\text{rad}}}{\rho_0 c S \langle V^2 \rangle}, \quad (14)$$

where the radiated sound power $\bar{\Pi}_{\text{rad}}$ is normalized by the product of the radiating surface area S , the characteristic impedance of the fluid $\rho_0 c$, where c is the speed of sound in the fluid, and the space-averaged mean square normal vibration velocity amplitude $\langle V^2 \rangle$ defined as

$$\langle V^2 \rangle = \frac{1}{2S} \iint_S |V|^2 dS. \quad (15)$$

By analogy with a lumped element system, the equivalent specific radiation resistance is $\rho_0 c \sigma_{\text{rad}}$.

3. Eigenanalysis of the Resistance Matrix

An important aspect of any Hermitian matrix is that it permits a useful decomposition of the matrix in terms of its eigenvalues and associated eigenvectors. This form of representation is commonly referred to as *eigenanalysis*.

The eigenvalue problem for the $N \times N$ resistance matrix \mathbf{R} is stated as

$$\mathbf{R}\mathbf{q}_i = \lambda_i \mathbf{q}_i, \quad i = 1, 2, \dots, N, \quad (16)$$

where λ_i denotes the i th eigenvalue of \mathbf{R} and \mathbf{q}_i is the nonzero eigenvector associated with λ_i . Equation (16) states that the vector \mathbf{q}_i is linearly transformed to the vector $\lambda_i \mathbf{q}_i$ by

the matrix \mathbf{R} . Now, let $\mathbf{q}_1, \mathbf{q}_2, \dots, \mathbf{q}_N$ be the eigenvectors corresponding to the distinct eigenvalues $\lambda_1, \lambda_2, \dots, \lambda_N$. Then, the eigenvectors satisfy

$$\mathbf{q}_i^H \mathbf{q}_j = \begin{cases} 1 & i = j, \\ 0 & i \neq j, \end{cases} \quad (17)$$

and they form an *orthonormal* set. The condition that $\mathbf{q}_i^H \mathbf{q}_i = 1$ requires that each eigenvector be normalized to have a unit length.

Now, we can see that the volume velocity vectors $\mathbf{u} \in \mathbb{C}^N$, where \mathbb{C}^N denotes a complex vector space of dimension N , and where N is the number of small elements in which the structure is divided. We can define this complex vector space as the set of complex vectors that can all be expressed as a linear combination of N basis vectors. So, specifically, we can write that $\mathbb{C}^N = \{\mathbf{y}\}$, where \mathbf{y} is any complex vector defined by

$$\mathbf{y} = \sum_{i=1}^N \alpha_i \mathbf{q}_i, \quad (18)$$

where the α_i are scalars. Therefore, the *dimension* N of the complex vector space \mathbb{C}^N is the minimum number of basis vectors required to span the entire space. Now, we say that \mathcal{S} is a *subspace* of the complex vector space \mathbb{C}^N if it involves a *subset* of the N basis vectors that define \mathbb{C}^N . In other words, a subspace of dimension k is defined as the set of volume velocities that can be written as a linear combination of the basis vectors $\mathbf{q}_1, \mathbf{q}_2, \dots, \mathbf{q}_k$, as shown by

$$\mathbf{u} = \sum_{i=1}^k \alpha_i \mathbf{q}_i. \quad (19)$$

Obviously, we have $k \leq N$, but the dimension of the vector \mathbf{u} is N .

Now, let the eigenvalues of \mathbf{R} be arranged in ascending order as $\lambda_1 \leq \lambda_2 \leq \dots \leq \lambda_N$. If the vector \mathbf{u} is constrained to lie in a subspace \mathcal{S} of dimension k , we can express the *Rayleigh quotient* of the vector \mathbf{u} as

$$\frac{\mathbf{u}^H \mathbf{R} \mathbf{u}}{\mathbf{u}^H \mathbf{u}} = \frac{\sum_{i=1}^k \alpha_i^2 \lambda_i}{\sum_{i=1}^k \alpha_i^2}. \quad (20)$$

Equation (20) states that the Rayleigh quotient of \mathbf{u} lying in the subspace \mathcal{S} of dimension k is a weighted mean of the eigenvalues. We can identify the numerator of Eq. (20) as twice the radiated sound power $\bar{\Pi}_{\text{rad}}$ and the denominator as a quantity proportional to the square of the velocity in the structure. Therefore, comparing with Eq. (14), Eq. (20) is identified as a quantity proportional to the sound radiation efficiency of the sound source. A similar equation has been presented by Cunefare *et al.*³⁹ for the structural *modal* radiation resistance matrix.

Now, by assumption, we have $\lambda_1 \leq \lambda_2 \leq \dots \leq \lambda_N$. Therefore, the *minimax theorem* for our application is

$$\lambda_k = \min_{\dim(\mathcal{S})=k} \max_{\substack{\mathbf{u} \in \mathcal{S} \\ \mathbf{u} \neq \mathbf{0}}} \frac{\mathbf{u}^H \mathbf{R} \mathbf{u}}{\mathbf{u}^H \mathbf{u}}, \quad k = 1, 2, \dots, N. \quad (21)$$

In general, for problems involving the sound radiation from vibrating structures, $k = N$ and then the subspace \mathcal{S} occupies the complex vector space \mathbb{C}^N entirely. Under this condition, Eq. (21) reduces to

$$\lambda_N = \max_{\substack{\mathbf{u} \in \mathbb{C}^N \\ \mathbf{u} \neq \mathbf{0}}} \frac{\mathbf{u}^H \mathbf{R} \mathbf{u}}{\mathbf{u}^H \mathbf{u}}, \quad (22)$$

where λ_N is the largest eigenvalue of the resistance matrix \mathbf{R} .

3.1. Extremization of the sound power

The minimax theorem is completely equivalent to the results obtained using an extremization of the sound power. The quadratic expression for the sound power given by Eq. (11) can produce a velocity vector in which the sound power radiated is an *extreme*. Assume we want to minimize Eq. (11) subject to the constraint $1/2 \mathbf{u}^H \mathbf{u} = g$, where g is some constant that ensures a bounded solution. Then, the Lagrange multiplier theorem can be used to find the solution of the constrained optimization problem. The Lagrange multiplier theorem states that with a velocity vector for which the sound power is stationary, the gradient of the Lagrangian functional L has to be zero. Now, the Lagrangian is

$$L = \frac{1}{2} \mathbf{u}^H \mathbf{R} \mathbf{u} - \bar{\lambda} \left(\frac{1}{2} \mathbf{u}^H \mathbf{u} - g \right), \quad (23)$$

where $\bar{\lambda}$ is the Lagrange multiplier.

Expanding the vector \mathbf{u} in terms of its real and imaginary parts as $\mathbf{u} = \mathbf{u}_r + j \mathbf{u}_i$ and substituting in Eq. (23) we can write the Lagrangian as

$$L = \frac{1}{2} (\mathbf{u}_r^H \mathbf{R} \mathbf{u}_r + \mathbf{u}_i^H \mathbf{R} \mathbf{u}_i) - \bar{\lambda} \left[\frac{1}{2} (\mathbf{u}_r^H \mathbf{u}_r + \mathbf{u}_i^H \mathbf{u}_i) - g \right]. \quad (24)$$

Differentiating Eq. (24) with respect to the real and the imaginary parts of \mathbf{u} , and equating the resultant expressions to zero, we obtain

$$\frac{\partial L}{\partial \mathbf{u}_r} = \mathbf{R} \mathbf{u}_r - \bar{\lambda} \mathbf{u}_r = 0, \quad (25)$$

and

$$\frac{\partial L}{\partial \mathbf{u}_i} = \mathbf{R} \mathbf{u}_i - \bar{\lambda} \mathbf{u}_i = 0. \quad (26)$$

Now, multiplying Eq. (26) by j and adding to Eq. (25) results in

$$\mathbf{R}\mathbf{u} = \bar{\lambda}\mathbf{u}, \quad (27)$$

which is the eigenvalue problem of Eq. (16). Therefore, the Lagrange multipliers $\bar{\lambda}$ correspond to the eigenvalues λ , and the vectors \mathbf{u} satisfying Eq. (27) are the eigenvectors \mathbf{q} .

Equations (22) and (27) present results which can be used in a low-frequency model. If a structure is vibrating with a surface velocity proportional to one of the eigenvectors of the matrix \mathbf{R} , then the vibration corresponds to a single radiation mode. In such a case, we can expect that for frequencies up to approximately the first resonance, the radiation efficiencies of the structure will be proportional to the eigenvalues of \mathbf{R} . Therefore, in order to calculate the radiation efficiencies of the radiation modes, we can reduce the amount of data to be stored in the memory of a computer, just by retaining the first eigenvalues for each frequency, since we will not need all the elements of the resistance matrix in this frequency range. Of course, this implies that we must perform an eigendecomposition of the matrix \mathbf{R} at low frequencies. However, if the structure is excited with several velocity distributions, this decomposition will need to be carried out just once. In addition, some functions provided in numerical programs allow the efficient computation of a few eigenvalues and eigenvectors of a square matrix.⁴⁰

3.2. Properties of the resistance matrix

To measure or calculate the matrix \mathbf{R} can be a difficult task, since a large number of elements are necessary for good precision. However, using some properties of the resistance matrix, this task can be simplified. For example, from Eq. (11), we can observe that $\bar{\Pi}_{\text{rad}}$ is a positive quantity, for all $\mathbf{u} \neq 0$, so that the matrix \mathbf{R} is a symmetric positive definite matrix.

In addition, if \mathbf{R} has a zero element on its main diagonal (R_{ii}), then the entire row and column to which it belongs must be zero. To reduce the computation time, it is also useful to analyze the behavior of the entries R_{ik} . If \mathbf{R} contains a significant number of zero elements, the computation time can be reduced. In performing matrix computations, the numerical programs normally assume that a matrix is dense, that is to say, any element in a matrix may be nonzero. The number of zero elements in a matrix is characterized by the *sparsity* of the matrix. A sparse matrix can be stored as a linear array of its nonzero elements along with their row and column indices. In the case of a sparse banded matrix, the storage can be done by specifying each diagonal. Using this approach, less memory is required if only the nonzero elements of the matrix are stored. This increase in efficiency in time and storage can make the solution of significantly larger problems feasible.

Another important observation is that the matrix \mathbf{R} can be decomposed as

$$\mathbf{R} = \mathbf{Q}^T \mathbf{\Lambda} \mathbf{Q}, \quad (28)$$

where \mathbf{Q} is a real unitary matrix of eigenvectors \mathbf{q}_i and $\mathbf{\Lambda}$ is a diagonal matrix of positive real eigenvalues λ_i . Then, $\bar{\Pi}_{\text{rad}}$ from Eq. (11) can be written as

$$\bar{\Pi}_{\text{rad}} = \frac{1}{2} \mathbf{u}^H \mathbf{Q}^T \mathbf{\Lambda} \mathbf{Q} \mathbf{u} = \frac{1}{2} \mathbf{y}^H \mathbf{\Lambda} \mathbf{y}, \quad (29)$$

where $\mathbf{y} = \mathbf{Q} \mathbf{u}$ is a vector of radiation modes in terms of the individual elements. Therefore, Eq. (29) can be written as

$$\bar{\Pi}_{\text{rad}} = \frac{1}{2} \sum_{i=1}^N \lambda_i |y_i|^2 = \frac{1}{2} \boldsymbol{\lambda}^T |\mathbf{y}|^2. \quad (30)$$

Equation (30) shows that each surface velocity distribution radiates sound independently, which means that they are uncoupled in terms of their radiation.^{15,32}

The advantage of writing the sound power radiated in the form of Eq. (30) is that the amplitudes of the radiation modes are defined directly in terms of the motion of an array of elements over the surface of the radiating body, without any reference to any structural mode amplitudes. The shapes of the radiation modes are thus given directly by the rows of the matrix \mathbf{Q} , which correspond to the eigenvectors of the resistance matrix \mathbf{R} . This representation gives a clearer physical insight into the mechanisms of control, and also had suggested an efficient implementation for an active control system, particularly at low frequencies.⁴¹

Now, if the structure is vibrating with a surface velocity proportional to one of the eigenvectors of the matrix \mathbf{R} , let us say \mathbf{q}_i , the surface velocity must be entirely in-phase or out-of-phase. That means that the vibration corresponds to a single radiation mode. Bai and Tsao³⁵ have identified these modes as evanescent modes (small λ_i), existing only in the near field, and propagating modes (large λ_i) that propagate efficiently into far field.

It is important to notice, however, that the shapes of the structural modes change when different sets of boundary conditions are selected, but the shapes of the velocity distributions that radiate sound independently do not.⁴¹

3.3. Numerical evaluation of the resistance matrix

As discussed before, the sound power radiated by a baffled vibrating plate can be expressed in terms of the volume velocities of a number of elemental radiators. However, most of the mesh used to discretize the plates are straight-sided geometrical forms, and the cross-impedances are given in terms of complex integral forms. However, if the vibrating plane structure (plate) is divided into N small virtual elements, each surface element can be treated as a circular piston having an area equal to that of the corresponding element. Hashimoto called this approach the *discrete calculation method* and used it experimentally to obtain the radiation efficiencies for several rectangular plates.⁴² Using this approach, the values for the self-resistance and cross-resistance are given by

$$R_{ii} = \rho_0 c S_i \left[1 - \frac{J_1(2k_0 a_i)}{k_0 a_i} \right], \quad (31)$$

and

$$R_{ik} = \frac{2\rho_0 c k_0^2 S_i S_k}{\pi} \left[\frac{J_1(k_0 a_i)}{k_0 a_i} \frac{J_1(k_0 a_k)}{k_0 a_k} \right] \text{sinc}(k_0 r_{ik}), \quad (32)$$

respectively, where c is the speed of sound, k_0 is the acoustic wavenumber, S_i and S_k are the surfaces of the equivalent pistons, $a_i = \sqrt{S_i/\pi}$ and $a_k = \sqrt{S_k/\pi}$ are the radii of the pistons, J_1 is the first-order Bessel function, and $\text{sinc}(x) = \sin(x)/x$. A theoretical derivation of Eq. (32) can be found in the work of Stepanishen.⁴³ If two pistons of equal area are assumed, it can be seen that an increase in the distance between the pistons results in a decrease in the cross-resistance which adopts more negative values at low frequencies.

For $x \ll 1$, we can approximate the first-order Bessel function using

$$J_1(x) \sim \frac{x}{2} - \frac{(x)^3}{16}. \quad (33)$$

Now, if the areas of each elementary radiator are assumed to be equal, then for very low frequencies ($k_0 a_i \ll 1$) we can substitute Eq. (33) into Eqs. (31) and (32). Retaining the terms up to quadratic order in the final result, and normalizing with respect to the area of each elementary radiator, we obtain

$$R_{ik} \sim \frac{\rho_0 c}{2\pi} k_0^2, \quad (34)$$

for all $i, k = 1, 2, \dots, N$.

4. Application to a Circular Baffled Plate

In order to test the performance of the method presented above, numerical simulations were carried out for a vibrating baffled circular plate. The use of circular plates in engineering structures is widespread and a large body of literature has been devoted to its study.^{44,45} The vibration of a circular plate's surface and its interaction with the fluid medium results in the radiation of sound and a coupled vibro-acoustic problem. Therefore, the resistance matrix combined with the volume velocity vector on the discretized circular plate's surface appears to be an efficient method to predict its sound radiation characteristics.

Now, to simplify the implementation of the computational codes, the circular disk could be divided into small elements of equal area. Transformation to a classical polar coordinate system will produce surface elements of different area. Therefore, if we divide the surface of a disk of radius a into N equally spaced concentric rings, it is possible to divide each ring into elements of equal area $\Delta S = (a/N)^2 \pi/4$. Thus, the new polar coordinates (r_i, θ_i) of the center point of each element ΔS are given as

$$r_i = \frac{a}{2N}(2i-1) \quad \text{and} \quad \theta_i = \frac{\pi(2j-1)}{4(2i-1)}, \quad (35)$$

where $i = 1, 2, \dots, N$ and $j = 1, 2, \dots, 4(2i-1)$. This discretization produces a $4N^2 \times 1$ vector \mathbf{u} and a $4N^2 \times 4N^2$ matrix \mathbf{R} .

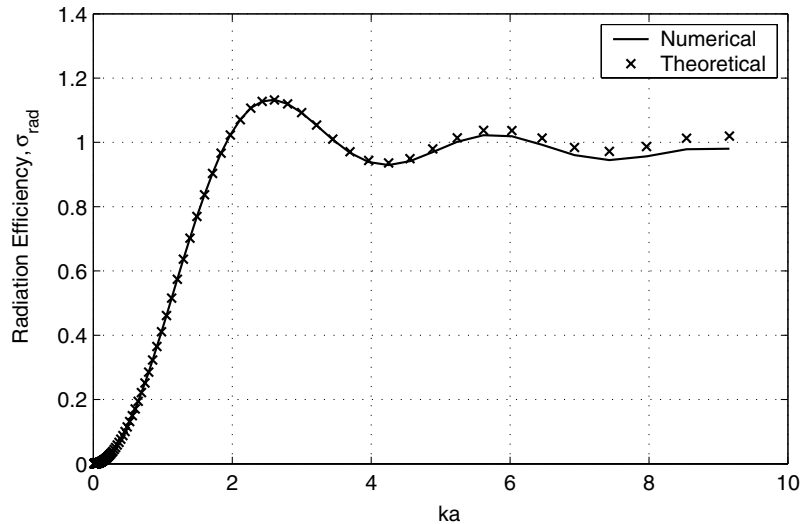


Fig. 2. Radiation efficiency of a baffled plane circular piston calculated theoretically and numerically using 400 elements.

In addition, if we assume a circular plate of radius a (total surface πa^2), and divided into M equal small elements, we can write $\langle V^2 \rangle$ using Eq. (15) as

$$\langle V^2 \rangle = \frac{M}{2\pi^2 a^4} \sum_{j=1}^M |u_j|^2 = \frac{M}{2\pi^2 a^4} \mathbf{u}^H \mathbf{u}. \quad (36)$$

The radiation efficiencies of both the radiation modes and some axisymmetric structural modes of a circular plate were numerically evaluated. Clamped and simply-supported boundary conditions were considered for the numerical examples. The circular plate was divided into 10 concentric rings, and so a total of 400 elements were considered. This number of elements was selected by comparison of the numerical results with the well-known radiation resistance of a baffled circular plane piston.³⁸ Figure 2 presents the comparison. The numerical results were obtained assuming that all the discrete points on the circular plate vibrate in-phase and with the same amplitude. It is observed that the numerical results compare quite well with the theoretical expression. The agreement is complete for $k_0 a \leq 4$. For $4 \leq k_0 a \leq 10$, the error does not exceed 3.5%. All the calculations were performed using a program written in Matlab[®]. Since the resistance matrix is frequency-dependent, it was evaluated as a hypermatrix in order to reduce the computation time.

4.1. Radiation modes

Using the eigenanalysis of the matrix \mathbf{R} , the characteristics of the radiation modes were evaluated for a baffled circular plate of radius a .

The radiation efficiencies, corresponding to the eigenvalues λ_i of the matrix \mathbf{R} , are plotted as a function of $k_0 a$ in Fig. 3. It is observed that, at low frequencies $k_0 a \ll 1$, the

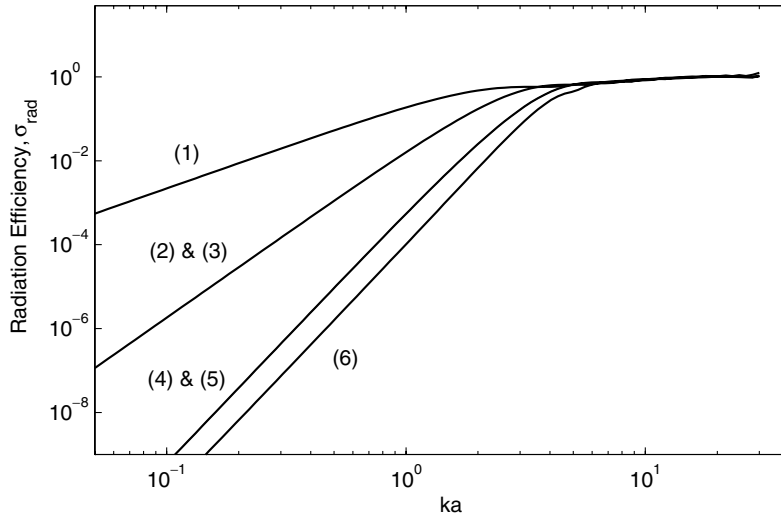


Fig. 3. Radiation efficiencies (eigenvalues λ_i of the matrix \mathbf{R}) of the first six radiation modes of a circular baffled plate.

first order (1) radiation mode is much more efficient at sound radiation than the higher order modes. For small values of k_0a , the radiation efficiency of the radiation modes fall off very rapidly with increasing mode order. This suggest that controlling the first-order radiation mode will produce a large reduction in the total sound power radiated. In addition, the grouping of some radiation modes can be observed in Fig. 3 due to the symmetry of the circular plate.

The velocity distribution of each radiation mode, corresponding to the eigenvectors \mathbf{q}_i of the matrix \mathbf{R} , are plotted in Fig. 4, for an excitation frequency corresponding to $k_0a = 0.1$. However, these velocity distributions are weak functions of the excitation frequencies and almost independent of the excitation frequency for $k_0a \ll 1$. It can be observed that the most efficient velocity distribution (1) clearly corresponds to the net volume displacement of the circular plate. Thus, radiation mode (1) is a piston mode which corresponds to a uniform weighting of all the points on the circular plate. Modes (2) and (3) are two rocking modes, one in each direction. The other modes have quadratic variations in both directions.

The results presented in Fig. 3 allow one to quantify the extent to which other velocity distributions are also radiating significantly at any one excitation frequency. It has been established that the number of structural modes that would have to be measured and controlled by an active system may be much greater than the number of radiation modes that would have to be controlled, at low frequencies.⁴⁶

4.2. Radiation from the structural axisymmetric modes

Now, the sound radiation efficiencies of a clamped and simply-supported circular plate of radius a vibrating in their structural axisymmetric natural modes were evaluated

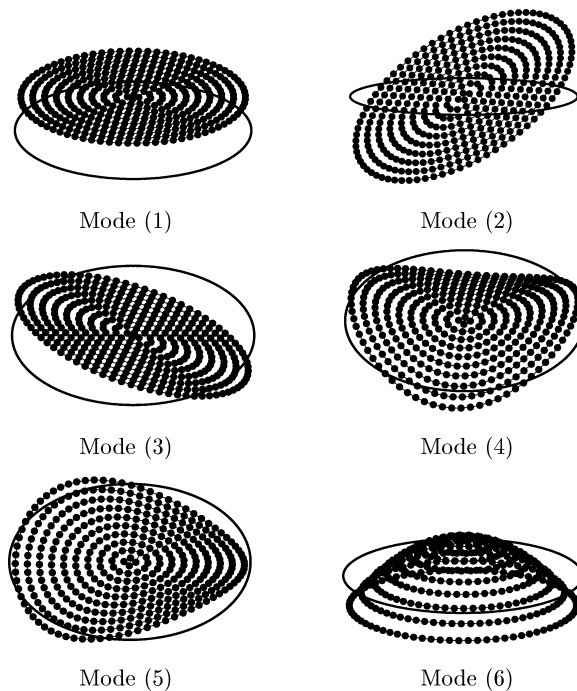


Fig. 4. Velocity distributions that radiate sound independently (eigenvectors \mathbf{q}_i of the matrix \mathbf{R}) of the first six radiation modes of a circular baffled plate. As a reference, the circles indicate the boundary of $\mathbf{q}_i = \mathbf{0}$.

numerically. The axisymmetric free vibration of an undamped thin circular plate is represented by the normal velocity mode function⁴⁷

$$V_n(r) = V_{0n} \left\{ J_0(k_n r) - \frac{J_0(\beta)}{I_0(\beta)} I_0(k_n r) \right\}, \quad (37)$$

where r is the radial distance from the plate center, V_{0n} is a constant velocity amplitude, J_0 and I_0 are cylinder functions, $k_n = k_p = \beta/a$ is the structural wavenumber, and $\beta = a\sqrt{\omega}(\rho/D)^{1/4}$ are the roots of the frequency equation

$$J_0(\beta)I_1(\beta) + J_1(\beta)I_0(\beta) = \begin{cases} 0 & \text{for clamped rim,} \\ \frac{2\beta}{1-\nu} J_0(\beta)I_0(\beta) & \text{for simply-supported rim,} \end{cases} \quad (38)$$

where ρ is the mass density per unit area of the plate, $D = Eh^3/12(1 - \nu^2)$ is the flexural rigidity, E is the modulus of elasticity (Young's modulus), h is the plate thickness, and ν is Poisson's ratio.

Of course, Eq. (37) has been developed assuming light fluid loading, so that the plate response is not affected by the surrounding environment, which acts as added mass and also provides radiation damping. From experimental observations this assumption is valid for vibrating structures in air but not valid for submerged structures. Loading by liquid

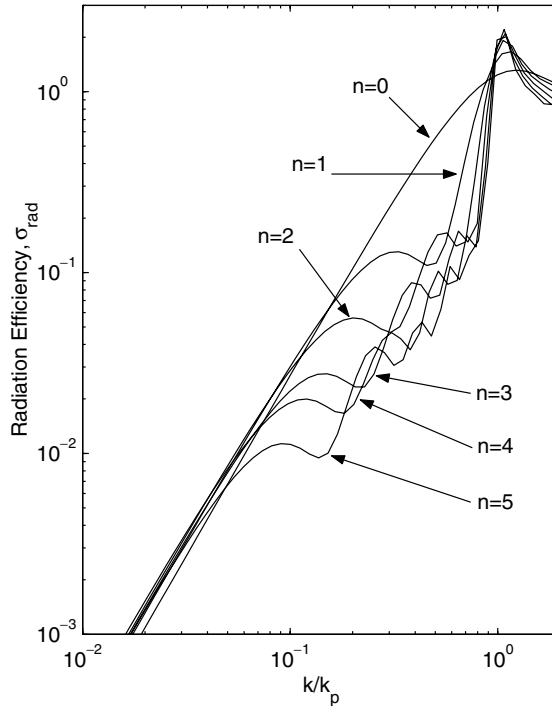


Fig. 5. Radiation efficiency for a number of axisymmetric modes of a clamped circular plate.

significantly lowers the natural frequencies of flat plates, the effect decreasing with increasing mode order.

Figure 5 shows the results for the radiation efficiency of the first six axisymmetric modes for a clamped plate predicted using Eqs. (11), (14), (36), and (37). Figure 6 presents the same results for a simply-supported plate. The results are plotted as a function of the dimensionless ratio between the acoustic wavenumber k_0 and the structural wavenumber k_p . Therefore, k_0/k_p is a measure of the critical frequency, where the propagation speed of the bending wave in the plate equals the speed of sound in the air. Thus, when $k_0/k_p < 1$ (subsonic wave) the mode is below the critical frequency and when $k_0/k_p > 1$ (supersonic wave) it is above.

The results in Figs. 5 and 6 are in good agreement with those presented by other authors which they determined from integral methods and asymptotic approximations.^{47,48} At $k_0/k_p = 1$, each sound radiation efficiency curve exhibits a peak, the height increasing with the axisymmetric mode numbers, and the efficiency reaches values greater than unity. The physical explanation of this fact has been discussed for rectangular plates in the literature.⁴⁹ However, we observe that well above the critical frequency the radiation efficiency curves for all the axisymmetric modes do not approach unity as theoretically expected. Clearly, this is because the method is discrete in nature. In order to improve the estimation, a larger number of elementary radiators should be considered, making the process very expensive in computation time. Therefore, for frequencies above the critical

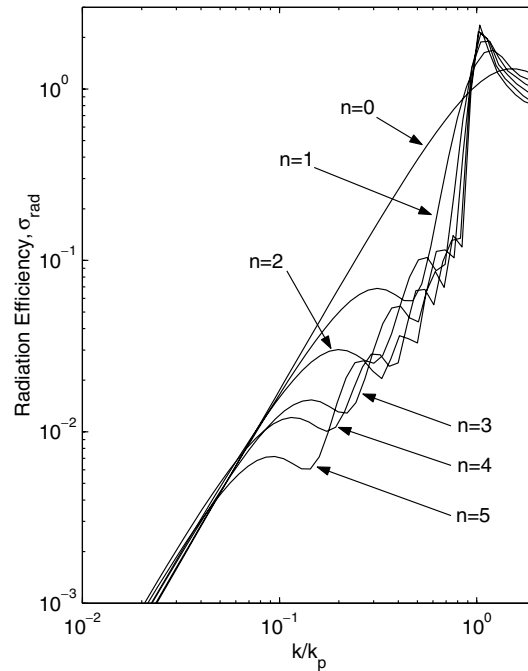


Fig. 6. Radiation efficiency for a number of axisymmetric modes of a simply-supported circular plate.

frequency, the use of well-known asymptotic approximations of the Rayleigh integral is more efficient.^{47,48}

In addition, it is observed that for frequencies well below the critical frequency, the efficiency of the first axisymmetric mode is large compared with the efficiencies of all the other modes. This implies that controlling the vibration of the first mode is a useful method of reducing the sound radiated at low frequencies. This is particularly practical for thin plates and plates submerged in water since the critical frequency for these cases is much higher and thus this region covers a broader range of frequencies.

However, it has to be noticed that these curves are applicable when the circular plate response is dominated by one mode, that is to say, at resonance. When the response of more than one mode is significant (off-resonance condition), the radiation efficiency requires more complex analysis. As in the case of rectangular plates, we should expect that when the total response of the plate is considered (including the contributions of all the modes), the radiation efficiency of a clamped circular plate should be less than the radiation efficiency of a simply-supported one for frequencies below the first resonance and larger for the mid-frequency range. Because of the asymptotic behavior of the radiation efficiency above the critical frequency, the radiation efficiencies will tend to be the same.

5. Conclusions

The characteristics of the sound radiation from a circular baffled plate have been numerically determined using the lumped parameter model. The results show good agreement

with previous theoretical and experimental results. The method reviewed here is very useful in the modeling of vibro-acoustic problems. The method can be combined with vibration measurements to predict the radiated sound power without measuring the sound field itself leading to interesting gain time factors. In addition, knowledge of the resistance matrix can be useful at the design stage, if numerical methods to compute the vibration response of a structure are combined with the resistance matrix to predict the sound power radiated. The method is limited to the frequencies below the critical frequency. For higher frequencies, a large number of virtual elements would be needed to obtain accurate prediction. Thus, for frequencies above the critical frequency, the use of asymptotic approximations is recommended.

Acknowledgments

This work was supported by Dir. de Investigación y Desarrollo DID-UACH under grant S-2005-01 and by FONDECYT grant No 1060117.

References

1. F. J. Blom, A monolithical fluid-structure interaction algorithm applied to the piston problem, *Comput. Methods Appl. Mech. Eng.* **167** (1998) 369.
2. Z. Fan, Transient vibration and sound radiation of a rectangular plate with viscoelastic boundary supports, *Int. J. Numer. Meth. Eng.* **51** (2001) 619.
3. N. Atalla and R. J. Bernhard, Review of numerical solutions for low-frequency structural-acoustic problems, *Appl. Acoust.* **43** (1994) 271.
4. R. D. Ciskowski and C. A. Brebbia, *Boundary Element Methods in Acoustics* (Elsevier, London, 1991).
5. J. B. Fahnlne, Condensing structural finite element meshes into acoustic element meshes, in *Proc. Design Engineering Technical Conf.*, Vol. 3B (ASME, 1995), pp. 641-646.
6. J. T. Chen, K. H. Chen and C. T. Chen, Adaptive boundary element method of time-harmonic exterior acoustics in two dimensions, *Comput. Methods Appl. Mech. Eng.* **191** (2002) 3331.
7. M. A. Tournour and N. Atalla, Efficient evaluation of the acoustic radiation using multipole expansion, *Int. J. Numer. Meth. Eng.* **46** (1999) 825.
8. M. J. Crocker and J. P. Arenas, Fundamentals of the direct measurement of sound intensity and practical applications, *Acoust. Phys.* **49** (2003) 163.
9. H. Lee and R. Singh, Acoustic radiation from out-of-plane modes of an annular disk using thin and thick plate theories, *J. Sound Vib.* **282** (2005) 313.
10. H. Lee and R. Singh, Comparison of two analytical methods used to calculate sound radiation from radial vibration modes of a thick annular disk, *J. Sound Vib.* **285** (2005) 1210.
11. S. M. Kirkup, Computational solution of the acoustic field surrounding a baffled panel by the Rayleigh integral method, *Appl. Math. Model.* **18** (1994) 403.
12. H. W. Wodtke and J. S. Lamancusa, Sound power minimization of circular plates through damping layer placement, *J. Sound Vib.* **215** (1998) 1145.
13. E. H. Paddock and G. H. Koopmann, The use of radiation resistance measurements to assess the noise characteristics of machines, in *Proc. Design Engineering Technical Conf.*, Vol. 3B (ASME, 1995), pp. 655-662.
14. A. Preumont, P. De Man and A. Francois, Some issues related to the feedback control of a baffled plate, *J. Struct. Control* **9** (2002) 153.

15. G. V. Borgiotti, The power radiated by a vibrating body in an acoustic fluid and its determination from boundary measurements, *J. Acoust. Soc. Am.* **88** (1990) 1884.
16. D. M. Photiadis, The relationship of singular value decomposition to wave-vector filtering in sound radiation problems, *J. Acoust. Soc. Am.* **88** (1990) 1152.
17. A. Sarkissian, Acoustic radiation from finite structures, *J. Acoust. Soc. Am.* **90** (1991) 574.
18. K. A. Cunefare, The minimum multimodal radiation efficiency of baffled finite beams, *J. Acoust. Soc. Am.* **90** (1991) 2521.
19. K. A. Cunefare and M. N. Currey, On the exterior acoustic radiation modes of structures, *J. Acoust. Soc. Am.* **96** (1994) 2302.
20. K. A. Cunefare, The design sensitivity and control of acoustic power radiated by three-dimensional structures, PhD dissertation, The Pennsylvania State University (1990).
21. P. T. Chen and J. H. Ginsberg, Complex power, reciprocity, and radiation modes for submerged bodies, *J. Acoust. Soc. Am.* **98** (1995) 3343.
22. J. B. Fahnline and G. H. Koopmann, A lumped parameter model for the acoustic power output from a vibrating structure, *J. Acoust. Soc. Am.* **100** (1996) 3539.
23. J. B. Fahnline and G. H. Koopmann, Numerical implementation of the lumped parameter model for the acoustic power output of a vibrating structure, *J. Acoust. Soc. Am.* **102** (1997) 179.
24. S. Marburg, Developments in structural-acoustic optimization for passive noise control, *Arch. Comput. Methods Eng.* **9** (2002) 291.
25. G. Hubner, A consideration of the physics of acoustic radiation (in German), *Acustica* **75** (1991) 130.
26. C. Maury and S. J. Elliott, Analytic solutions of the radiation modes problem and the active control of sound power, *Proc. Roy. Soc. A* **461** (2005) 55.
27. D. Fritze, S. Marburg and H. J. Hardtke, Reducing radiated sound power of plates and shallow shells by local modification of geometry, *Acta Acustica United with Acustica* **89** (2003) 53.
28. A. Kuijpers, Acoustic modeling and design of MRI scanners, PhD dissertation, Technische Universiteit Eindhoven (1999).
29. P. H. L. Kessels, Engineering toolbox for structural-acoustic design. Applied to MRI scanners, PhD dissertation, Technische Universiteit Eindhoven (2001).
30. K. Naghshineh and G. H. Koopmann, Active control of sound power using acoustic basis functions as surface velocity filters, *J. Acoust. Soc. Am.* **93** (1993) 2740.
31. W. T. Baumann, F. S. Ho and H. H. Robertshaw, Active structural acoustic control of broadband disturbances, *J. Acoust. Soc. Am.* **92** (1992) 1998.
32. S. J. Elliott and M. E. Johnson, Radiation modes and the active control of sound power, *J. Acoust. Soc. Am.* **94** (1993) 2194.
33. M. N. Currey and K. A. Cunefare, The radiation modes of baffled finite plates, *J. Acoust. Soc. Am.* **98** (1994) 1570.
34. A. P. Berkhoff, Sensor scheme design for active structural acoustic control, *J. Acoust. Soc. Am.* **108** (2000) 1037.
35. M. R. Bai and M. Tsao, Estimation of sound power of baffled planar sources using radiation matrices, *J. Acoust. Soc. Am.* **112** (2002) 876.
36. J. P. Arenas and M. J. Crocker, Sound radiation efficiency of a baffled rectangular plate excited by harmonic point forces using its surface resistance matrix, *Int. J. Acoust. Vib.* **7** (2002) 217.
37. P. M. Morse and K. U. Ingard, *Theoretical Acoustics* (Princeton University Press, Princeton, 1986).
38. A. D. Pierce, *Acoustics: An Introduction to Its Physical Principles and Applications* (Acoustical Society of America, New York, 1989).
39. K. A. Cunefare, M. N. Currey, M. E. Johnson and S. J. Elliott, The radiation efficiency grouping of free-space acoustic radiation modes, *J. Acoust. Soc. Am.* **109** (2001) 203.

40. R. B. Lehoucq, D. C. Sorensen and C. Yang, *ARPACK Users' Guide: Solution of Large-Scale Eigenvalue Problems with Implicitly Restarted Arnoldi Methods* (SIAM Publications, Philadelphia, 1998).
41. S. J. Elliott, *Signal Processing for Active Control* (Academic Press, London, 2001).
42. N. Hashimoto, Measurement of sound radiation efficiency by the discrete calculation method, *Appl. Acoust.* **62** (2001) 429.
43. P. R. Stepanishen, Evaluation of mutual radiation impedances between circular pistons by impulse response and asymptotic methods, *J. Sound Vib.* **59** (1978) 221.
44. G. W. Wei, A new algorithm for solving some mechanical problems, *Comput. Methods Appl. Mech. Eng.* **190** (2001) 2017.
45. T. Y. Wu, Y. Y. Wang and G. R. Liu, Free vibration analysis of circular plates using generalized differential quadrature rule, *Comput. Methods Appl. Mech. Eng.* **191** (2002) 5365.
46. M. E. Johnson and S. J. Elliott, Active control of sound radiation using volume velocity cancellation, *J. Acoust. Soc. Am.* **98** (1995) 2174.
47. H. Levine and F. G. Leppington, A note on the acoustic power output of a circular plate, *J. Sound Vib.* **121** (1988) 269.
48. W. Rdzanek, The sound power of a circular plate for high-frequency wave radiation, *Archives Acoust.* **3** (1983) 331.
49. E. G. Williams, *Fourier Acoustics: Sound Radiation and Nearfield Acoustic Holography* (Academic Press, San Diego, 1999).